



McIntyre, C. L., Monin, L., Rop, J. C., Otto, T. D., Goodyear, C. S., Hayday, A. C. and Morrison, V. L. (2020) $\beta 2$ integrins differentially regulate $\gamma\delta$ T cell subset thymic development and peripheral maintenance. *Proceedings of the National Academy of Sciences of the United States of America*, 117(36), pp. 22367-22377. (doi: [10.1073/pnas.1921930117](https://doi.org/10.1073/pnas.1921930117)).

This is the author's final accepted version.

There may be differences between this version and the published version. You are advised to consult the publisher's version if you wish to cite from it.

<http://eprints.gla.ac.uk/222339/>

Deposited on: 11 September 2020

Enlighten – Research publications by members of the University of Glasgow
<http://eprints.gla.ac.uk>

β_2 integrins differentially regulate $\gamma\delta$ T cell subset thymic development and peripheral maintenance

Claire L. McIntyre,¹ Leticia Monin,² Jesse C. Rop,¹ Thomas D. Otto,¹ Carl S. Goodyear,¹ Adrian C. Hayday,^{2,3} and Vicky L. Morrison^{1*}.

¹Institute of Infection, Immunity & Inflammation, University of Glasgow, Glasgow, G12 8TA, UK.

²Immunosurveillance Laboratory, The Francis Crick Institute, London, NW1 1AT, UK.

³Peter Gorer Dept of Immunobiology, King's College London, London, WC2R 2LS, UK.

*Corresponding author: Dr Vicky L. Morrison, University of Glasgow, SGDB room B612, 120 University Place, Glasgow, G12 8TA; 0141 330 8791; vicky.morrison@glasgow.ac.uk

Classification

Biological Sciences; Immunology and Inflammation

Keywords

β_2 integrins, $\gamma\delta$ T cells, immune homeostasis

Author Contributions

C.L.M. and V.L.M. designed the project. C.L.M., L.M. and V.L.M. performed the experiments and analyzed the data. J.C.R. developed the online platform for visualizing the sequencing data. T.D.O. analyzed the sequencing data. C.S.G. and A.H. provided valuable contribution to the direction of the project. C.L.M. and V.L.M. wrote the manuscript with input from all co-authors.

This PDF file includes:

Main Text
Figures 1 to 6
SI Appendix

Abstract

$\gamma\delta$ T cells reside predominantly at barrier sites and play essential roles in immune protection against infection and cancer. Despite recent advances in the development of $\gamma\delta$ T cell immunotherapy, our understanding of the basic biology of these cells, including how their numbers are regulated *in vivo*, remains poor. This is particularly true for tissue-resident $\gamma\delta$ T cells. We have identified the β_2 family of integrins as novel regulators of $\gamma\delta$ T cells. β_2 integrin-deficient mice displayed a striking increase in numbers of IL-17-producing V γ 6V δ 1⁺ $\gamma\delta$ T cells in the lungs, uterus and circulation. Thymic development of this population was normal. However, single cell RNA sequencing revealed the enrichment of genes associated with T cell survival and proliferation specifically in β_2 integrin-deficient IL-17⁺ cells compared to their WT counterparts. Indeed, β_2 integrin-deficient V γ 6⁺ cells from the lungs showed reduced apoptosis *ex vivo*, suggesting that increased survival contributes to the accumulation of these cells in β_2 integrin-deficient tissues. Furthermore, our data revealed an unexpected role for β_2 integrins in promoting the thymic development of the IFN γ -producing CD27⁺ V γ 4⁺ $\gamma\delta$ T cell subset. Together, our data reveal that β_2 integrins are important regulators of $\gamma\delta$ T cell homeostasis, inhibiting the survival of IL-17-producing V γ 6V δ 1⁺ cells and promoting the thymic development of the IFN γ -producing V γ 4⁺ subset. Our study indicates new and unprecedented mechanisms of control for $\gamma\delta$ T cell subsets.

Significance Statement

$\gamma\delta$ T cells reside in barrier tissues and provide immune protection against infection and cancer. Their anti-tumor potential has led to recent advances in the development of $\gamma\delta$ T cell immunotherapy. However, our understanding of the basic biology of these cells, including what molecules and pathways control their maintenance within barrier tissues, remains poor. We demonstrate that β_2 integrin adhesion molecules play a major role in regulating $\gamma\delta$ T cell subset numbers during homeostasis: the loss of β_2 integrin expression results in a striking increase in IL-17-producing $\gamma\delta$ T cells in the lungs and uterus due to enhanced survival. These findings illustrate a novel mechanism of $\gamma\delta$ T cell regulation that may have significant implications for immunotherapy development.

Main Text

Introduction

$\gamma\delta$ T cells are innate-like cells that play essential roles in immune surveillance, neonatal immunity and responses to infection and tumors. Tissue-resident $\gamma\delta$ T cells localize within barrier sites such as the skin, gut, lungs, genital tract and oral mucosa, enabling rapid responses against infectious challenge without the need for clonal expansion. Upon recognition of foreign antigens, host stress-induced markers or innate-derived cytokines (1-3), $\gamma\delta$ T cells mediate immune protection via direct killing of target cells and production of pro-inflammatory cytokines, IFN γ and IL-17.

$\gamma\delta$ T cells are the major innate source of IL-17 during the early phase of an immune response (4). Mouse models have demonstrated protective roles for IL-17-producing $\gamma\delta$ T cells in a range of mucosal infections (5-7). In humans, IL-17-producing $\gamma\delta$ T cells have been reported in cord blood (8) and can be expanded from PBMCs *in vitro* (9, 10). Although their contribution to infection-driven immune responses remains poorly described, IL-17-producing $\gamma\delta$ T cell numbers are increased in patients with bacterial meningitis (10), suggesting an important role.

We set out to explore the regulatory roles of β_2 integrins in $\gamma\delta$ T cell populations that reside in barrier tissues. β_2 integrins are leukocyte-specific adhesion molecules that consist of the β_2 chain (CD18) coupled to CD11a (α_L), CD11b (α_M), CD11c (α_X) or CD11d (α_D). It is well characterized that Leukocyte Function-associated Antigen-1 (LFA-1; CD11a/CD18) is essential for many aspects of $\alpha\beta$ T cell function (11): by binding intercellular adhesion molecules (ICAMs) on endothelial cells LFA-1 mediates T cell recruitment to lymph nodes (LN) and sites of inflammation; LFA-1 localizes to the immunological synapse between interacting T and antigen-presenting cells, stabilizing contacts and lowering the threshold for T cell activation; T cell LFA-1 mediates interactions with target cells (e.g. B cells or cancerous/infected cells) facilitating effector T cell functions. However, the involvement of β_2 integrins in $\gamma\delta$ T cell recruitment, interactions and function is less well defined (reviewed in (12)). Whilst some reports demonstrate a role for β_2 integrins in mediating $\gamma\delta$ T cell interactions with endothelial cells (13), $\gamma\delta$ T cell trafficking to sites of inflammation can occur independently of β_2 integrins, as shown in multiple sclerosis (14) and psoriasis (15) models.

Evidence suggests that β_2 integrins control $\gamma\delta$ T cell numbers and/or localization: under conditions of skin and periodontal inflammation in CD18-deficient (CD18^{hypo} PL/J) and CD11a knockout (KO) mice, respectively, increased numbers of $\gamma\delta$ T cells were found at inflamed sites (15, 16). Even in the absence of overt inflammation, increased proportions and/or numbers of $\gamma\delta$ T cells have been reported in the cervical LNs (17), spleen and mesenteric LNs (18) of CD18 KO mice. Based on this evidence, we hypothesized that β_2 integrins regulate $\gamma\delta$ T cell numbers during homeostasis and inflammation. However, these studies have been limited in the tissues analyzed, making it unclear if the alterations in cell number are due to expansion or redistribution. Additionally, $\gamma\delta$ T cell numbers, subset profiles and phenotype at barrier sites (e.g. lungs, small intestine, uterus, gingiva), where these cells have major immune protective roles, have not been analyzed in β_2 integrin-deficient mice.

In this study we investigated the impact of β_2 integrin-deficiency on $\gamma\delta$ T cell subset numbers, localization and phenotype. We demonstrate that loss of β_2 integrin expression leads to a tissue-restricted increase in IL-17-producing V γ 6V δ 1⁺ $\gamma\delta$ T cells that is prominent in the lungs, uterus and spleen. We also reveal a novel role for β_2 integrins in promoting thymic development of IFN γ -producing CD27⁺ V γ 4⁺ $\gamma\delta$ T cells.

Results

β_2 integrin-deficient mice have a tissue-restricted increase in $\gamma\delta$ T cells

$\gamma\delta$ T cell numbers were quantified in a range of lymphoid and mucosal tissues from β_2 integrin-deficient (CD18 KO) mice. $\alpha\beta$ T cells were analyzed for comparison. $\gamma\delta$ T cell numbers were increased in the lungs, uterus, spleen and blood of CD18 KO mice, whereas numbers in the skin (includes both dermis and epidermis), oral mucosa, gut and other lymphoid tissues were unaffected by β_2 integrin loss (Fig. 1; gating shown in SI Appendix, Fig. S1). As anticipated, $\alpha\beta$ T cell numbers were reduced in the LNs, Peyer's patches and bone marrow, as a result of defective homing (19, 20). Importantly, we saw no reduction in $\gamma\delta$ T cell numbers in any of the tissues analyzed, indicating

that the increase in $\gamma\delta$ T cells in CD18 KO mice is not due to redistribution but, instead, a tissue-specific expansion.

β_2 integrin loss leads to an increase in IL-17-producing $\gamma\delta$ T cells

$\gamma\delta$ T cells are broadly divided into two mutually exclusive phenotypes based on cytokine profile: IFN γ -producing cells and IL-17-producing cells. Splenic $\gamma\delta$ T cells from CD18 KO mice produced significantly higher levels of IL-17 as both proportion and absolute numbers compared to WT cells (Fig. 2A-B). Increased IL-17 was observed across the tissues where $\gamma\delta$ T cell numbers were increased (Fig. 2B). The enhanced numbers of IL-17-producing $\gamma\delta$ T cells in CD18 KO mice contributed to an increase in serum IL-17 levels (SI Appendix, Fig. S2A-B). Despite the apparent defect in the percentage of IFN γ -producing CD18 KO $\gamma\delta$ T cells (Fig. 2A), the number of IFN γ -producing $\gamma\delta$ T cells was equivalent (Fig. 2B).

The expanded $\gamma\delta$ T cell population in β_2 integrin-deficient mice express the V γ 6V δ 1 TCR

Next, we questioned whether the expanded $\gamma\delta$ T cell population was due to an increase in one or more $\gamma\delta$ T cell subsets in β_2 integrin-deficient mice. Murine $\gamma\delta$ T cell subsets express different V γ chains, numbered V γ 1-7 (Heilig and Tonegawa nomenclature (21)), which localize to specific tissues and have different capacity for cytokine production (22). We predicted that CD18 KO mice would have an increase in V γ 4⁺ and/or V γ 6⁺ $\gamma\delta$ T cells, as these subsets are the predominant IL-17-producers (23). V γ chain expression was initially analyzed using antibodies against V γ 1, V γ 4 and V γ 5. Despite proportional differences in multiple subsets (SI Appendix, Fig. S3A), calculation of absolute numbers revealed a significant increase only in the V γ 1⁺V γ 4⁻V γ 5⁻ $\gamma\delta$ T cells in CD18 KO mice (Fig. 2C). This was true for all tissues where an increase was previously found in total $\gamma\delta$ T cell numbers (Fig. 1 and Fig. 2C). PCR analysis of the 'unknown' V γ 1⁺V γ 4⁻ population in CD18 KO mice revealed expression of the V γ 6 and V δ 1 TCR chains (Fig. 2D; SI Appendix, Fig. S3B). Note that although V γ 2 is expressed at the mRNA level, protein expression does not correlate with in-

frame transcript expression, and high RNA level may reflect poor allelic exclusion (24). Extensive flow cytometric analysis confirmed that CD18 KO splenic $\gamma\delta$ T cells displayed a marker phenotype consistent with IL-17-producing cells: they were predominantly CD62L^{lo}, CD44^{hi}, CD27⁻, CD45RB⁻ and Ror γ t⁺ (SI Appendix, Fig. S3C), suggestive of IL-17 production (25, 26); and they expressed higher levels of CD3 and TCR $\gamma\delta$ than their WT counterparts (SI Appendix, Fig. S3C), a phenotype that implies a V γ 6-expressing phenotype (27). Together, these data show that the absence of β_2 integrin expression leads to an increase in IL-17-producing $\gamma\delta$ T cells that express the V γ 6V δ 1 TCR.

The increase in IL-17-producing $\gamma\delta$ T cells is due to loss of LFA-1

β_2 integrins are a family of four receptors, the loss of one or more of which could cause the $\gamma\delta$ T cell expansion seen in CD18 KO mice. Analysis of CD11 chain KO mice revealed that the increase in $\gamma\delta$ T cell numbers was due to the specific loss of LFA-1, as increased numbers of $\gamma\delta$ T cells were detected in the spleen and lungs of CD11a KO mice but not in mice lacking CD11b, CD11c or CD11d (SI Appendix, Fig. S4A). We confirmed that the enhanced capacity to produce IL-17 was also observed in the expanded $\gamma\delta$ T cell population in CD11a KO mice (SI Appendix, Fig. S4B).

Thymic development of V γ 6⁺ $\gamma\delta$ T cells is unaffected by β_2 integrin loss, whilst CD27⁺V γ 4⁺ $\gamma\delta$ T cell development is impaired

We next sought to investigate the mechanism of expansion of V γ 6⁺ IL-17-producing $\gamma\delta$ T cells in β_2 integrin-deficient mice. V γ 6⁺ $\gamma\delta$ T cells egress from the thymus from embryonic 16.5 (E16.5) to a few days after birth and are, thereafter, maintained in the periphery by self-renewal (28). Analysis of the thymus showed equivalent numbers of V γ 6⁺ $\gamma\delta$ T cells in WT and CD18 KO mice in embryonic, neonatal (1 and 3 day old), and adult (4 week old) mice (Fig. 3A). As thymic output of V γ 6⁺ cells both at the peak of development and in adult mice was normal, we conclude that the development of V γ 6⁺ cells is not influenced by β_2 integrin deficiency.

Surprisingly, whilst V γ 1⁺ and V γ 5⁺ $\gamma\delta$ T cell development was also equivalent in WT and CD18 KO mice, we found a reduction in the number of thymic V γ 4⁺ $\gamma\delta$ T cells in embryonic and neonatal mice (Fig. 3A). Further analysis to differentiate between immature and mature populations revealed that the reduced number of total V γ 4⁺ cells was due to a loss of immature CD24⁺ cells at E18.5, and then mature CD24⁻ V γ 4⁺ cells in 4 week old mice (Fig. 3B). This suggests that the loss of β_2 integrin expression impairs V γ 4⁺ $\gamma\delta$ T cell development from the early, immature stage. The number of V γ 6⁺ cells, regardless of maturation status, was similar in the thymus of WT and CD18 KO mice, further confirming that V γ 6⁺ $\gamma\delta$ T cell development is unaffected by β_2 integrin loss.

IL-17- and IFN γ -producing $\gamma\delta$ T cells can be distinguished by expression of CD27, which is present only on IFN γ -producers (25). Further analysis revealed that numbers of CD27⁺ V γ 4⁺ cells in the thymus were reduced in CD18 KO mice across all ages of mice analyzed (Fig. 3C). No differences were found in CD27⁻ V γ 4⁺ cells. These data suggest that β_2 integrin loss causes a specific defect in the development of CD27⁺ V γ 4⁺ $\gamma\delta$ T cells that have the potential to produce IFN γ .

To determine whether this impaired development impacts on the numbers of V γ 4⁺ cells in the periphery, tissues were analyzed in adult mice. We previously showed that the number of V γ 4⁺ cells was equivalent in CD18 KO mice at sites where the expanded V γ 6⁺ cells were found (lungs, uterus, spleen and blood) (Fig. 2C). However, as V γ 4⁺ cells commonly reside within lymphoid tissues, we performed a more thorough examination. The number of V γ 4⁺ cells was significantly decreased in the peripheral LNs (inguinal, brachial and axillary pooled). A similar trend of reduced V γ 4⁺ cell numbers was observed in the mediastinal LN and bone marrow, but this did not reach statistical significance (Fig. 3D). These findings indicate that the impaired development of V γ 4⁺ $\gamma\delta$ T cells in CD18 KO mice results in reduced numbers of these cells specifically in the peripheral LNs.

Single cell sequencing reveals evidence of enhanced survival of β_2 integrin-deficient V γ 6⁺ cells

Next, single cell RNA sequencing (scRNAseq) was used to investigate the possible mechanism(s) by which β_2 integrins control $\gamma\delta$ T cell numbers in the periphery. Principal component analysis of lung $\gamma\delta$ T cells revealed 5 biologically distinct clusters: the *Il17a*⁺ cluster which contains both $V\gamma 6^+$ (*Cd163l1*⁺ *Trdv4*⁺) and $V\gamma 4^+$ (*5830411N06Rik*⁺) cells, two *Cd27*⁺ clusters namely *Ccr7*⁺ and *Ly6c2*⁺, and much smaller clusters of killer cells (*Gzma*⁺) and dividing cells (*Cdk6*⁺) (Fig. 4A; SI Appendix, Fig. S5A-C). As expected, the CD18 KO cells were over-represented in the *Il17a*⁺ cluster (Fig. 4B). High expression of the $V\gamma 6$ (*Tcrg-V6*) and $V\delta 1$ (*Trdv4*) TCR subunits as well as *Scart1* (*Cd163l1*), confirmed the expanded CD18 KO population as $V\gamma 6^+$ cells (SI Appendix, Fig. S5D). The number of differentially expressed (DE) genes when comparing WT to KO was much greater in the *Il17a*⁺ cluster (1439 genes) than the *Ccr7*⁺ (74 genes) or *Ly6c2*⁺ (32 genes) clusters (Fig. 4C; Dataset S1A-C). We determined the DE genes that were unique to the IL-17-producing population (Fig. 4C; Dataset S2), excluding DE genes dependent on the loss of the β_2 integrin which were common to 2 or 3 of the dominant $\gamma\delta$ T cell populations. Pathway analysis revealed enrichment of genes associated with T cell activation, survival and proliferation in CD18 KO cells from the IL-17-producing cluster (Fig. 4D; SI Appendix, Fig. S5E; Dataset S3). Specifically, the pro-survival genes *Bcl2a1a* and *Bcl2a1d*, known to support the survival of skin-resident $V\gamma 6^+$ cells (29), were uniquely enriched in CD18 KO *Il17a*⁺ $\gamma\delta$ T cell cluster (Fig. 4E; SI Appendix, Fig. S5E). Other genes reported to enhance survival in T cells (TCR subunits and signaling molecules, the IL-2 receptor, *Cd44* and *Icos*) as well as in cancer cells (*Crip1*) (30) were also enriched in the CD18 KO *Il17a*⁺ cluster (Fig. 4E; SI Appendix, Fig. S5E). Together, scRNAseq analysis revealed the dysregulation of pathways involved in cell survival and proliferation specifically in the CD18 KO IL-17-producing $\gamma\delta$ T cell population.

Cell survival, rather than proliferation, is the dominant driver of $V\gamma 6^+$ $\gamma\delta$ T cell accumulation in β_2 integrin-deficient mice

Assessing proliferation *in vivo*, we detected a small but significant increase in Ki67 expression in V γ 6⁺ cells from both the spleen and lungs of CD18 KO mice compared to WT (Fig. 5A). However, we found similar incorporation of BrdU by WT or CD18 KO V γ 6⁺ or V γ 4⁺ cells in either tissue over the 7-day period of analysis (Fig. 5B), suggesting that β ₂ integrin-deficient V γ 6⁺ cells do not show enhanced proliferation in adult mice. This data is supported by the scRNAseq analysis which shows that CD18 KO cells are not enriched in the dividing *Cdk6*⁺ cluster (Fig. 4B), and by GO enrichment analysis where pathways associated with apoptosis dominated (Fig. 4D).

Next, we sought to determine whether cell survival is influenced by β ₂ integrin deficiency. Detailed analysis of tissues from CD18 KO mice of various ages revealed that V γ 6⁺ $\gamma\delta$ T cell numbers in the lungs and spleen were equivalent to WT mice at E18.5, when this population begins to egress the thymus (Fig. 6A; SI Appendix, Fig. S6A). However, at 1-day post-birth, CD18 KO mice show increased numbers of V γ 6⁺ $\gamma\delta$ T cells in the lungs, and from 3-day old mice onwards, the numbers in the spleen were also elevated. Interestingly, whilst V γ 6⁺ $\gamma\delta$ T cell numbers in the lungs reach a plateau from day 3, numbers in the spleen of CD18 KO mice continue to rise as the mice age, increasing to 40-fold more than WT at 4 weeks (Fig. 6A). Surface marker analysis confirmed that the expanded $\gamma\delta$ T cell population displayed the expected CD45RB⁻ CD44⁺ CD27⁻ phenotype consistent with IL-17-producing potential (SI Appendix, Fig. S6B). These data indicate that the increased number of V γ 6⁺ $\gamma\delta$ T cells initially arise in the lungs and then the spleen. The accumulation of cells over time is consistent with enhanced V γ 6⁺ cell survival in CD18 KO mice.

IL-7 is known to drive T cell survival through Bcl2 (31). As *Il7r* was expressed at higher levels in CD18 KO cells compared to WT in the *Il17a*⁺ cluster (SI Appendix, Fig. S5D) and “cellular response to IL-7” was a hit in pathway analysis (Dataset S3), we assessed expression of IL-7R and Bcl2 in lung $\gamma\delta$ T cells. Expression of IL-7R was higher in V γ 6⁺ cells compared to V γ 4⁺ cells but was equivalent between WT and CD18 KO cells (SI Appendix, Fig. S7A). Bcl2 expression was also equivalent in WT and CD18 KO $\gamma\delta$ T cells (SI Appendix, Fig. S7B). Thus, signaling through the IL-7R-Bcl2 axis is not elevated in β ₂ integrin-deficient $\gamma\delta$ T cells.

Next, we investigated the effect of β_2 integrin loss on $\gamma\delta$ T cell survival by direct *ex vivo* analysis. $V\gamma 6^+$ $\gamma\delta$ T cells from the lungs of CD18 KO mice displayed reduced apoptosis compared to WT, with increased proportion of live cells and reduced proportion of late apoptotic cells (Fig. 6B). This effect was specific to the $V\gamma 6^+$ cells, as the proportions of live and apoptotic cells in the $V\gamma 4^+$ population were equivalent. Furthermore, the enhanced survival of CD18 KO cells was specific to the lungs, as cells in the spleen showed similar levels of apoptosis regardless of genotype or subset (Fig. 6B). Of note, this enhanced survival was most apparent in 4-week-old mice (Fig. 6C) as well as adult mice (Fig. 6B), whereas viability of $V\gamma 6^+$ cells in neonatal mice was equivalent in WT and CD18 KO mice (Fig. 6C). Thus, the enhanced survival of lung $V\gamma 6^+$ cells, particularly in adult mice, likely contributes to the accumulation of this $\gamma\delta$ T cell subset in CD18 KO mice.

LFA-1 expression is higher in $V\gamma 6^+$ cells compared to $V\gamma 4^+$ cells, particularly in the lungs, in WT mice

Finally, we questioned why β_2 integrin loss led to the selective expansion of the $V\gamma 6^+$ subset. Assessment of β_2 integrin expression in $\gamma\delta$ T cells revealed only CD11a (LFA-1) and not CD11b or CD11c expression (SI Appendix, Fig. S8). In the lungs, expression of CD11a was highest in the $V\gamma 6^+$ population compared to $V\gamma 1^+$ and $V\gamma 4^+$ cells, whereas $\gamma\delta$ T cell populations expressed equivalent, lower levels of CD11a in the spleen (Fig. 6C). CD11a expression was equivalent across $\gamma\delta$ T cell populations in the pLN (SI Appendix, Fig. S8) where $V\gamma 6^+$ cell numbers are unaffected by CD18 deficiency (Fig. 3D). These data suggest that $V\gamma 6^+$ $\gamma\delta$ T cells in the lungs may be most affected by β_2 integrin loss as this population express the highest levels of LFA-1.

Discussion

In this study we reveal that the absence CD18 expression in mice leads to a striking increase in $V\gamma 6V\delta 1^+$ IL-17-producing $\gamma\delta$ T cell numbers in the lungs and uterus, as well as the blood and

spleen. V γ 6⁺ cells showed no difference in thymic development or proliferation but displayed a transcriptional profile consistent with enhanced survival and reduced levels of apoptosis *ex vivo*. Surprisingly, we also found that β ₂ integrin loss impaired the development of IFN γ -producing (CD27⁺) V γ 4⁺ $\gamma\delta$ T cells, leading to reduced numbers of this subset in peripheral LNs. Together, our findings highlight novel roles for β ₂ integrins in promoting V γ 4⁺ $\gamma\delta$ T cell development and in negatively regulating V γ 6⁺ $\gamma\delta$ T cell numbers in the periphery via apoptosis. In doing so, β ₂ integrins alter the balance between IL-17- and IFN γ -producing $\gamma\delta$ T cells at mucosal and lymphoid sites.

Importantly, we found no defect in $\gamma\delta$ T cell numbers in any tissue, showing conclusively that the increase in $\gamma\delta$ T cell numbers reported here and in previous studies in integrin-deficient mice (17, 18) is not a redistribution effect but a tissue-specific increase in $\gamma\delta$ T cells that occurs in the absence of LFA-1. In agreement with previous studies (14, 15), our findings indicate that homing of $\gamma\delta$ T cells to an extensive range of mucosal and lymphoid tissues is not dependent on β ₂ integrins.

It was unsurprising that the increase in $\gamma\delta$ T cell numbers was most apparent in the lungs and uterus (in addition to the spleen), as V γ 6⁺ cells preferentially localize to these tissues (26, 32). However, V γ 6⁺ cells also reside in the dermis (33) and gingiva (34), where no differences were found. Analysis of whole skin (epidermis and dermis) may have masked any differences exclusive to the dermis. In addition, there may be stronger competition by other skin-resident T cells, precluding accumulation of V γ 6⁺ cells in the dermis. Alternatively, the expanded V γ 6⁺ $\gamma\delta$ T cell population in CD18 KO mice may be truly tissue specific. V γ 6⁺ cells are not described to preferentially home to the spleen, although they have been shown to reside there (26, 27). We propose that the increasing number of V γ 6⁺ cells exceeds the capacity within their resident tissues (lungs and uterus), which forces the $\gamma\delta$ T cells into the circulation and causes accumulation in the spleen. The enhanced number of $\gamma\delta$ T cells in the blood and appearance of increased numbers in the lungs prior to the spleen in newborn mice support this.

Analysis of CD18^{hyp} mice (CD18 expression at 2-16% of WT) revealed the expanded $\gamma\delta$ population in the skin to have a CD27⁻ IL-17⁺ phenotype (15). The authors reported expression of V γ 4 rather than V γ 6 in the majority (~50%) of cells, although markers for V γ 6⁺ cells were not assessed. The

potential difference in V γ chain expression in CD18 KO mice versus CD18^{hypo} mice could be due to genetic differences (C57BL/6J versus PL/J backgrounds), the level of CD18 expression (absent versus low), or changes induced by inflammation (no overt inflammation in our CD18 KO mice; severe dermatitis in the CD18^{hypo} mice (15)).

Although thymic development of V γ 6⁺ cells was unaffected by β ₂ integrin loss, we found an unexpected defect in V γ 4⁺ cell development. The defect was specific to the IFN γ -producing CD27⁺ V γ 4⁺ cells. The loss of CD18 impacts early in V γ 4⁺ $\gamma\delta$ T cell development (fewer immature V γ 4⁺ cells at E18.5) but is not absolutely necessary, as the V γ 4⁺ cells are reduced in number but not completely ablated. Interestingly, the numbers of V γ 4-expressing $\gamma\delta$ T cells were only reduced in the peripheral LNs of adult CD18 KO mice and not the spleen or lungs where this population also resides. This may indicate that migration of V γ 4⁺ cells to peripheral LNs is partially dependent on β ₂ integrins or that factors present in the spleen and lungs but absent in peripheral LNs preferentially expand or retain V γ 4⁺ cells. The functional consequences of the reduced numbers of V γ 4⁺ cells in peripheral LNs of CD18 KO mice remains to be determined. As IFN γ production by V γ 4⁺ cells is protective in models of melanoma (35, 36) and viral infection (37), reduced numbers of V γ 4⁺ cells may enhance pathology in these models.

Our study highlights survival, rather than proliferation, as the dominant mechanism of V γ 6⁺ cell accumulation in adult CD18 KO mice. We did find a slight but significant increase in Ki67 expression in V γ 6⁺ cells from CD18 KO mice, potentially indicating longer time spent in active cell cycle (38), whilst not progressing to proliferation. Indeed, by BrdU incorporation we found little evidence of active $\gamma\delta$ T cell proliferation regardless of genotype, which fits with published reports showing low turnover of V γ 6⁺ cells in adult mice (33, 39). Although it is possible that CD18 KO cells may be undergoing increased proliferation compared to WT at a slow rate not detected, the scRNAseq analysis shows a very small population of dividing (*Cdk6*⁺) $\gamma\delta$ T cells, the frequency of which is unaltered in CD18 KO mice. Whilst it remains possible that proliferation contributes to an increase in V γ 6⁺ cells in neonatal mice, our data illustrate that survival is the major contributor to V γ 6⁺ population expansion in β ₂ integrin-deficient mice from 4 weeks of age and in adult mice.

scRNAseq analysis of lung $\gamma\delta$ T cells revealed a striking enrichment of genes associated with survival, specifically in the β_2 integrin-deficient $V\gamma 6^+$ $\gamma\delta$ T cells. Importantly, *ex vivo* analysis confirmed that $V\gamma 6^+$ cells from the lungs of CD18 KO mice displayed decreased apoptosis compared to WT. Several TCR components as well as molecules downstream of the TCR signaling pathway (*Cd44*, *Icos*, *Lat*, *Nr4a1* (*Nur77*)) were increased in CD18 KO $V\gamma 6^+$ cells, suggesting that TCR signaling may contribute to the pro-survival phenotype. Although ligands that drive the expansion and retention of $V\gamma 5^+$ and $V\gamma 7^+$ $\gamma\delta$ T cells have been characterized, namely Skint1 (40) and Btl1 (41) respectively, a ligand specific for $V\gamma 6^+$ cells has not yet been identified. If such a ligand exists, an upregulation in CD18 KO lungs and uterus may contribute to the expansion phenotype seen in this study. Furthermore, two members of the Bcl2a1 family (*Bcl2a1a*, *Bcl2a1d*), that have been reported to support the survival of skin-resident $V\gamma 6^+$ cells (29), were also enhanced in our CD18 KO lung $V\gamma 6^+$ cells. Therefore, it is likely that a combination of signaling pathways that promote cell survival contribute to the accumulation of $V\gamma 6^+$ cells in β_2 integrin-deficient mice.

One remaining question is why the increase in $\gamma\delta$ T cells is restricted to the $V\gamma 6$ -expressing subset. β_2 integrins expressed by $\gamma\delta$ T cells may contribute directly to the induction of apoptosis (42). As we found LFA-1 expression to be highest in $V\gamma 6^+$ cells in the lungs, this may explain the specificity of survival of the $V\gamma 6^+$ subset in LFA-1-deficient mice.

Although not definitive from our study, a cell-intrinsic role for LFA-1 in suppressing $\gamma\delta$ T cell apoptosis is supported by the following evidence: (i) $\gamma\delta$ T cell expansion was dependent on the loss of LFA-1 but no other β_2 integrin family members; (ii) in our hands, $\gamma\delta$ T cells highly expressed LFA-1 but no other CD11 subunits; (iii) the expansion of $\gamma\delta$ T cells was apparent in the tissues of CD18 KO mice from 1 day post-birth when other lymphocyte populations are still developing (e.g. very few $\alpha\beta$ T cells are present); and (iv) the increase in $\gamma\delta$ T cells was first observed in the lungs where stromal populations (negative for LFA-1) rather than leukocytes predominate. We, therefore, propose a model where LFA-1, potentially in conjunction with TCR and/or death receptor signaling, contributes to the induction of apoptosis in $V\gamma 6^+$ $\gamma\delta$ T cells.

The functional consequences of the expanded IL-17-producing $\gamma\delta$ T cell population in β_2 integrin-deficient mice remain to be determined. IL-17-producing $\gamma\delta$ T cells are known to be required for effective pathogen clearance, particularly in the lungs and uterus (5-7, 43), and yet contribute to pathology in models of autoimmune disorders (44, 45) and cancer (46). We would predict that the expanded $V\gamma 6^+$ cell population will alter outcome in these immune challenge models in an IL-17-dependent manner.

Although a subset equivalent to the $V\gamma 6^+$ $\gamma\delta$ T cells identified in mice does not exist in humans, future analysis of $V\delta 1$ - and $V\delta 2$ -expressing subsets, both of which have been shown to produce IL-17, may reveal a potential role for β_2 integrins in regulating specific subsets of human $\gamma\delta$ T cells. The targeting of IL-17-producing $\gamma\delta$ T cells has been identified as a therapeutic strategy for patients with spondyloarthritis (47), therefore further work to elucidate the role of β_2 integrins in the regulation human $\gamma\delta$ T cells may reveal novel targets for therapy.

In summary, our findings reveal unanticipated roles for the β_2 integrin, LFA-1, in regulating the balance between IL-17- and IFN γ -producing $\gamma\delta$ T cell subsets: β_2 integrins promote the development of IFN γ -producing CD27 $^+$ $V\gamma 4^+$ cells in the thymus, whilst suppressing the survival of IL-17-producing CD27 $^-$ $V\gamma 6^+$ cells in the periphery. The striking expansion of $V\gamma 6^+$ cells in β_2 integrin-deficient mice demonstrates the central role this integrin plays in regulating this elusive $\gamma\delta$ T cell population. The impact of these and other adhesion molecules on the survival and phenotype of $\gamma\delta$ T cells should be carefully considered when developing cancer therapeutics to target the immuno-protective functions of this lymphocyte population.

Materials and Methods

Mice

CD18 (#003329) KO mice were purchased from The Jackson Laboratory. Age and sex-matched mice were used in all experiments. C57BL/6J mice (Envigo) or transgenic negative littermates were

used as controls. Mice were housed at the University of Glasgow. All protocols were conducted under licenses issued by the U.K. Home Office under the Animals (Scientific Procedures) Act of 1986 and approved by the local ethics committee.

Tissue Processing

Single cell suspensions were prepared from spleen, thymus, mesenteric LNs, mediastinal LNs, peripheral LNs (inguinal, brachial and axillary pooled) and Peyer's patches by mashing between 45µm NITEX pieces (Cadisch Precision Meshes Ltd.). Cells were isolated from bone marrow by flushing using a 26G needle. Spleen, blood and bone marrow cell suspensions were lysed with RBC lysis buffer (eBioscience). Uterus' were digested using Multi Dissociation Kit 1 (Miltenyi Biotec) according to the manufacturer's instructions. Ear skin was digested in 2mg/ml Collagenase IV, 2mg/ml hyaluronidase (both Sigma-Aldrich), and 100 U/ml DNase I (Invitrogen) at 37°C for 40 min at 180 RPM in a rotating incubator, then dissociated using a gentlemacs (Miltenyi Biotec). The following tissues were digested as described: lungs(48), small intestine(49), gingiva(50). Cells were counted by trypan blue exclusion.

Flow cytometry

Details of flow cytometry antibodies can be found in the SI Appendix. Cells were stained with fixable viability dye eFluor506 (eBioscience) for 30mins at 4°C. Extracellular staining was performed in Fc block (supernatant from 2.4G2 cell line) for 30mins at 4°C. For intracellular cytokine staining, cells were stimulated with 10ng/ml PMA (Sigma Aldrich), 500ng/ml ionomycin (Sigma Aldrich) and 1:1000 GolgiPlug (BD Biosciences) for 4h at 37°C. Following extracellular staining, cells were fixed using Cytofix/Cytoperm and stained in Perm/Wash (both BD Biosciences). For transcription factor staining, cells were fixed using FoxP3 Transcription Factor Fixation/Permeabilisation buffer and stained in permeabilization buffer (both eBioscience). All intracellular staining was for 1hr at room temperature (RT). For apoptotic cell staining, cells were stained with AnnexinV (Biolegend) and 7AAD (BD Biosciences) in AnnexinV staining buffer (Biolegend) for 15mins at RT. All cells were re-

suspended in FACS buffer (PBS 2% FBS 2mM EDTA) and acquired on LSRII or LSR Fortessa (BD Biosciences). Data was analyzed using Flowjo software (Treestar).

Fluorescence-activated cell sorting

$\gamma\delta$ T cells from CD18 KO spleens were pre-enriched using EasySep™ Mouse T cell Isolation Kit (Stemcell Technologies). Live, CD3⁺TCR $\gamma\delta$ ⁺, V γ 1⁻V γ 4⁻ cells were then sorted using a FACS Aria IIU (BD Biosciences).

RNA isolation, cDNA and PCR

RNA was purified using RNeasy Mini Kit (Qiagen) according to the manufacturer's instructions. cDNA synthesis was carried out using High-Capacity RNA-to-cDNA Kit (Applied Biosystems). V γ and V δ chain sequences were amplified using 0.02U/ μ l, 1X Phusion HF buffer, 3% DMSO, 2mM MgCl₂ (V γ 6 reaction only) (all Thermo Fisher), 0.2mM dNTPs (Invitrogen) and 0.3 μ M primers (IDT Technologies). Primer sequences for V γ 1, V γ 4, V γ 5, V γ 6 and V γ 7 were kindly provided by Dr Pierre Vantourout (King's College London) and for V γ 2 and V δ have been described(51). DNA fragments were separated on 1% agarose (Invitrogen) gels and visualized using Gel Doc™ XR+ system (BioRad).

Single cell RNA sequencing

$\gamma\delta$ T cells were isolated from the lungs of 2 WT mice and 1 CD18 KO mouse by FACS-sorting for CD3⁺ TCR $\gamma\delta$ ⁺ cells. Single cell suspensions were loaded into a Chromium Controller (10X Genomics). Subsequently, cDNA was generated from polyadenylated RNA, amplified and converted to Illumina compatible libraries according to standard protocol published in Single Cell 3' Reagent Kits v3 User Guide (10X Genomics). These were sequenced on an Illumina NextSeq500 sequencer with a sequencing depth of approximately 50,000 read pairs per cell. The read 1 and 2 were 28bp and 91bp long, respectively. scRNAseq reads were mapped in Cellranger (version 3.1.0) (52) against the current *Mus musculus* reference (mm10-3.0.0). The obtained readcount matrixes were analyzed in Seurat (53), version 3.1.2 in R version 3.5.3. We followed the analysis as described in (54). To clean the data of doublets and dying cells, we filtered cells for a

mitochondria amount less than 18% and applied the nFeature_RNA a cut-off of 2200, 3200 and 2500 cells for WT1, WT2 and KO, respectively. To remove technical variation, we used the SCTransform protocol in Seurat. WT1 and KO samples were integrated first, and then WT2 added which was down sampled to 4000 cells. The number of PCA transformation dimensions was 15; and the “findcluster” resolution was 0.15. Marker genes were selected for cluster annotation, non-T cell clusters removed, and clustering then repeated. The default Seurat values (FindMarkers function) were used to determine differentially expressed (DE) genes, with an adjusted p-value cut-off of 0.01. Venny 2.1 (bioinfogp.cnb.csic.es/tools/venny/) was used to compare DE genes in different clusters. GO enrichment pathway analysis was performed in Panther (pantherdb.org/). The reads and read counts are available in ArrayExpress under the accession number E-MTAB-8732. Furthermore, we designed a cell atlas to query the data, which can be accessed via this link: <http://cellatlas.mvls.gla.ac.uk/gdT-cell/> This cell atlas was programmed in R-shiny using the Seurat pipeline as describe above.

Statistical analysis

Student’s *t* test or two-way ANOVA (Graphpad Prism) were used to calculate statistical significance. Sidak’s multiple comparisons test was used to correct for multiple comparison. P values shown as ns not significant, * $p < 0.05$, ** $p < 0.01$, *** $p < 0.005$, **** $p < 0.0001$.

Data Availability Statement

The reads and read counts from the single cell RNA sequencing are available in ArrayExpress (<https://www.ebi.ac.uk/arrayexpress/>) under the accession number E-MTAB-8732. All other data are included in the main text or *SI Appendix*. Further information about data and reagents used is available by request to the corresponding author.

Acknowledgments

We thank Drs Seth Coffelt and Sarah Edwards for critical reading of the manuscript; Prof Christie Ballantyne (Baylor College of Medicine, Texas, USA) for providing CD11c KO mice; Dr Pierre Vantarout (King's College London) for providing primer sequences; the Flow Cytometry Core Facility (University of Glasgow) for assistance with cell sorting; and the Central Research Facility (University of Glasgow) for assistance with timed matings; and Dr Pawel Herzyk and Julie Galbraith at Glasgow Polyomics research facility (University of Glasgow) for performing the single cell RNA sequencing. Portions of this paper were developed from C.L.M.'s PhD thesis. This work was supported by Versus Arthritis (to V.L.M.; 20848), The Carnegie Trust (to V.L.M.; RIG007542), Wellcome (to V.L.M.; 204820/Z/16/Z), 10X Genomics (to V.L.M.), and the European Union's Horizon 2020 research and innovation program (Marie Skłodowska-Curie grant to L.M.; 792383).

Competing Interest Statement

The authors declare no competing interest.

References

1. J. C. Ribot *et al.*, Cutting Edge: Adaptive Versus Innate Receptor Signals Selectively Control the Pool Sizes of Murine IFN- γ - or IL-17-Producing $\gamma\delta$ T Cells upon Infection. *The Journal of Immunology* **185**, 6421-6425 (2010).
2. A. C. Hayday, gammadelta T Cell Update: Adaptate Orchestrators of Immune Surveillance. *J Immunol* **203**, 311-320 (2019).
3. J. Strid *et al.*, Acute upregulation of an NKG2D ligand promotes rapid reorganization of a local immune compartment with pleiotropic effects on carcinogenesis. *Nat Immunol* **9**, 146-154 (2008).
4. C. E. Sutton *et al.*, Interleukin-1 and IL-23 induce innate IL-17 production from gammadelta T cells, amplifying Th17 responses and autoimmunity. *Immunity* **31**, 331-341 (2009).
5. N. D. Ritchie, R. Ritchie, H. K. Bayes, T. J. Mitchell, T. J. Evans, IL-17 can be protective or deleterious in murine pneumococcal pneumonia. *PLOS Pathogens* **14**, e1007099 (2018).
6. T. A. Moore, B. B. Moore, M. W. Newstead, T. J. Standiford, Gamma delta-T cells are critical for survival and early proinflammatory cytokine gene expression during murine Klebsiella pneumonia. *J Immunol* **165**, 2643-2650 (2000).

7. T. Dejima *et al.*, Protective Role of Naturally Occurring Interleukin-17A-Producing $\gamma\delta$ T Cells in the Lung at the Early Stage of Systemic Candidiasis in Mice. *Infection and immunity* **79**, 4503-4510 (2011).
8. E. Moens *et al.*, IL-23R and TCR signaling drives the generation of neonatal Vgamma9Vdelta2 T cells expressing high levels of cytotoxic mediators and producing IFN-gamma and IL-17. *J Leukoc Biol* **89**, 743-752 (2011).
9. M. L. Michel *et al.*, Interleukin 7 (IL-7) selectively promotes mouse and human IL-17-producing gammadelta cells. *Proc Natl Acad Sci U S A* **109**, 17549-17554 (2012).
10. N. Caccamo *et al.*, Differentiation, phenotype, and function of interleukin-17-producing human Vgamma9Vdelta2 T cells. *Blood* **118**, 129-138 (2011).
11. B. L. Walling, M. Kim, LFA-1 in T Cell Migration and Differentiation. *Front Immunol* **9**, 952 (2018).
12. G. M. Siegers, Integral Roles for Integrins in gammadelta T Cell Function. *Front Immunol* **9**, 521 (2018).
13. N. Mohagheghpour, L. E. Bermudez, S. Khajavi, A. Rivas, The VLA-4/VCAM-1 molecules participate in $\gamma\delta$ cell interaction with endothelial cells. *Cellular immunology* **143**, 170-182 (1992).
14. J. E. Wolher, S. S. Smith, K. R. Zinn, D. C. Bullard, S. R. Barnum, Gamma delta T cells in Experimental Autoimmune Encephalomyelitis: Early Trafficking Events and Cytokine Requirements. *Eur J Immunol.* **39**, 1516-1526 (2009).
15. M. Gatzka *et al.*, Reduction of CD18 promotes expansion of inflammatory gammadelta T cells collaborating with CD4+ T cells in chronic murine psoriasiform dermatitis. *J Immunol* **191**, 5477-5488 (2013).
16. N. Moutsopoulos *et al.*, Defective Neutrophil Recruitment in Leukocyte Adhesion Deficiency Type I Disease Causes Local IL-17-driven Inflammatory Bone Loss. *Sci Transl Med* **6**, 1-21 (2014).
17. T. Oreshkova *et al.*, B2 Integrin deficiency yields unconventional double-negative T cells distinct from mature classical natural killer T cells in mice. *Immunology* **128**, 271-286 (2009).
18. M. A. Stark *et al.*, Phagocytosis of apoptotic neutrophils regulates granulopoiesis via IL-23 and IL-17. *Immunity* **22**, 285-294 (2005).
19. C. Berlin-Rufenach *et al.*, Lymphocyte migration in lymphocyte function-associated antigen (LFA)-1-deficient mice. *J Exp Med* **189**, 1467-1478 (1999).
20. V. L. Morrison *et al.*, The beta2 integrin-kindlin-3 interaction is essential for T-cell homing but dispensable for T-cell activation in vivo. *Blood* **122**, 1428-1436 (2013).
21. J. S. Heilig, S. Tonegawa, Diversity of murine gamma genes and expression in fetal and adult T lymphocytes. *Letters to Nature* **322**, 836-840 (1986).
22. P. Vantourout, A. Hayday, Six-of-the-best: unique contributions of gammadelta T cells to immunology. *Nat Rev Immunol* **13**, 88-100 (2013).
23. R. L. O'Brien, M. Lahn, W. K. Born, S. A. Huber, T cell receptor and function cosegregate in gamma-delta T cell subsets. *Chem Immunol* **79**, 1-28 (2001).
24. P. Pereira *et al.*, Rearrangement and expression of Vy1, Vy2 and Vy3 TCR y genes in C57BL/6 mice. *International immunology* **8**, 83-90 (1996).

25. J. C. Ribot *et al.*, CD27 is a thymic determinant of the balance between interferon-gamma- and interleukin 17-producing gammadelta T cell subsets. *Nat Immunol* **10**, 427-436 (2009).
26. C. L. Roark *et al.*, Subset-specific, uniform activation among V gamma 6/V delta 1+ gamma delta T cells elicited by inflammation. *Journal of leukocyte biology* **75**, 68-75 (2004).
27. C. Paget *et al.*, CD3(bright) signals on $\gamma\delta$ T cells identify IL-17A-producing V γ 6V δ 1(+) T cells. *Immunology and cell biology* **93**, 198-212 (2014).
28. J. D. Haas *et al.*, Development of Interleukin-17-Producing $\gamma\delta$ T Cells Is Restricted to a Functional Embryonic Wave. *Immunity* **37**, 48-59 (2012).
29. L. Tan *et al.*, Single-Cell Transcriptomics Identifies the Adaptation of Scart1(+) Vgamma6(+) T Cells to Skin Residency as Activated Effector Cells. *Cell Rep* **27**, 3657-3671 e3654 (2019).
30. L. Zhang *et al.*, Cysteine-rich intestinal protein 1 suppresses apoptosis and chemosensitivity to 5-fluorouracil in colorectal cancer through ubiquitin-mediated Fas degradation. *J Exp Clin Cancer Res* **38**, 120 (2019).
31. K. Akashi, M. Kondo, U. Von Freeden-Jeffry, R. Murray, I. L. Weissman, Bcl-2 rescues T lymphopoiesis in Interleukin-7 receptor-deficient mice. *Cell* **89**, 1033-1041 (1997).
32. S. Itohara *et al.*, Homing of a gamma delta thymocyte subset with homogeneous T-cell receptors to mucosal epithelia. *Nature* **343**, 754-757 (1990).
33. Y. Cai *et al.*, Differential developmental requirement and peripheral regulation for dermal V γ 4 and V γ 6T17 cells in health and inflammation. *Nature communications* **5**, 3986 (2014).
34. A. Wilharm *et al.*, Mutual interplay between IL-17-producing $\gamma\delta$ T cells and microbiota orchestrates oral mucosal homeostasis. *Proceedings of the National Academy of Sciences* **116**, 2652-2661 (2019).
35. J. Hao *et al.*, Regulatory Role of V γ 1 $\gamma\delta$ T Cells in Tumor Immunity through IL-4 Production. *The Journal of Immunology* **187**, 4979-4986 (2011).
36. W. He *et al.*, Naturally Activated V γ 4 $\gamma\delta$ T Cells Play a Protective Role in Tumor Immunity Through Expression of Eomesodermin1. *J Immunol* **185**, 1-18 (2010).
37. J. Dodd, S. Riffault, J. S. Kodituwakku, A. C. Hayday, P. J. M. Openshaw, Pulmonary V gamma 4+ gamma delta T cells have proinflammatory and antiviral effects in viral lung disease. *Journal of immunology (Baltimore, Md. : 1950)* **182**, 1174-1181 (2009).
38. I. Miller *et al.*, Ki67 is a Graded Rather than a Binary Marker of Proliferation versus Quiescence. *Cell Reports* **24**, 1105-1112.e1105 (2018).
39. I. Sandrock *et al.*, Genetic models reveal origin, persistence and non-redundant functions of IL-17-producing $\gamma\delta$ T cells. *The Journal of experimental medicine* **215**, 3006-2018 (2018).
40. L. M. Boyden *et al.*, Skint1, the prototype of a newly identified immunoglobulin superfamily gene cluster, positively selects epidermal $\gamma\delta$ T cells. *Nature Genetics* **40**, 656-662 (2008).
41. R. Di Marco Barros *et al.*, Epithelia Use Butyrophilin-like Molecules to Shape Organ-Specific $\gamma\delta$ T Cell Compartments. *Cell* **167**, 203-218.e217 (2016).

42. Y. Matsumoto *et al.*, Co-stimulation with LFA-1 triggers apoptosis in gamma delta T cells on T cell receptor engagement. *Eur J Immunol* **24**, 2441-2445 (1994).
43. P. Cheng *et al.*, Role of gamma-delta T cells in host response against *Staphylococcus aureus*-induced pneumonia. *BMC Immunol* **13**, 38 (2012).
44. P. Kulig *et al.*, IL-12 protects from psoriasiform skin inflammation. *Nature communications* **7**, 13466 (2016).
45. A. Akitsu *et al.*, IL-1 receptor antagonist-deficient mice develop autoimmune arthritis due to intrinsic activation of IL-17-producing CCR2+V γ 6+ $\gamma\delta$ T cells. *Nature communications* **6**, 7464 (2015).
46. M. Rei *et al.*, Murine CD27(-) V γ 6(+) gammadelta T cells producing IL-17A promote ovarian cancer growth via mobilization of protumor small peritoneal macrophages. *Proc Natl Acad Sci U S A* **111**, E3562-3570 (2014).
47. K. Venken *et al.*, ROR γ inhibition selectively targets IL-17 producing iNKT and gammadelta-T cells enriched in Spondyloarthritis patients. *Nature communications* **10**, 9 (2019).
48. R. A. Benson, J. C. Lawton, M. K. L. Macleod, T Cell Response in the Lung Following Influenza Virus Infection. *Methods Mol Biol.* **1591**, 235-248 (2017).
49. S. a. Houston *et al.*, The lymph nodes draining the small intestine and colon are anatomically separate and immunologically distinct. *Mucosal immunology* **9**, 468-478 (2016).
50. G. Mizraji, H. Segev, A. Wilensky, A.-H. Hovav, Isolation, Processing and Analysis of Murine Gingival Cells. *Journal of Visualized Experiments* **77**, e50388 (2013).
51. E. M. Andrew *et al.*, Delineation of the function of a major gamma delta T cell subset during infection. *J Immunol* **175**, 1741-1750 (2005).
52. G. X. Zheng *et al.*, Massively parallel digital transcriptional profiling of single cells. *Nature communications* **8**, 14049 (2017).
53. A. Butler, P. Hoffman, P. Smibert, E. Papalexi, R. Satija, Integrating single-cell transcriptomic data across different conditions, technologies, and species. *Nat Biotechnol* **36**, 411-420 (2018).
54. T. Stuart *et al.*, Comprehensive Integration of Single-Cell Data. *Cell* **177**, 1888-1902 e1821 (2019).

Figure Legends

Fig. 1. CD18 KO mice have increased numbers of $\gamma\delta$ T cells in the lungs, uterus, spleen and blood. Cells were isolated from various lymphoid and mucosal tissues of WT (open circles) and CD18 KO (closed circles) mice then analyzed by flow cytometry. Skin includes both dermis and epidermis. Cells were gated on CD3⁺ then TCR β ⁺ or TCR $\gamma\delta$ ⁺ as shown in SI Appendix, Fig. S1. Absolute number of $\alpha\beta$ and $\gamma\delta$ T cells per tissue is shown. For blood, numbers were calculated per 100 μ l. SI = small intestine; mLN = mesenteric LNs; pLN = peripheral LNs (brachial, axillary and inguinal pooled). n=10, data pooled from a minimum of 3 independent experiments; each symbol

represents and individual mouse. Statistical differences were determined using a two-way ANOVA * $p < 0.05$, ** $p < 0.01$, **** $p < 0.0001$.

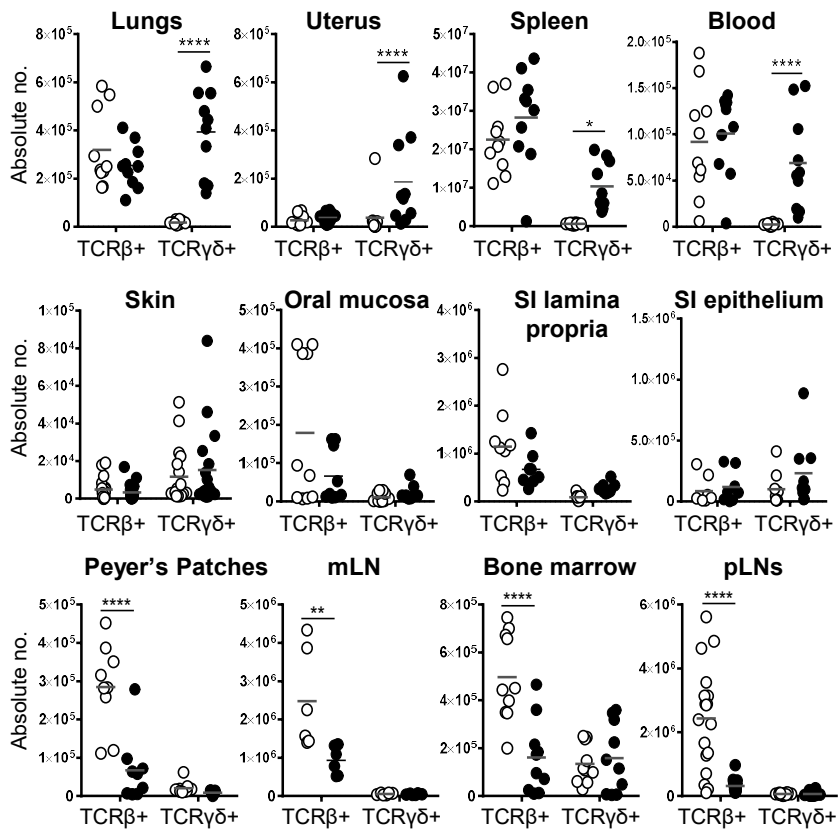
Fig. 2. IL-17-producing V γ 6V δ 1⁺ $\gamma\delta$ T cells are increased in CD18 KO mice. (A) Representative plot showing percentage of IL-17⁺ and IFN γ ⁺ $\gamma\delta$ T cells from WT and CD18 KO spleen following *in vitro* stimulation with PMA/ionomycin/BfA for 4h. (B) Number of IL-17⁺ and IFN γ ⁺ $\gamma\delta$ T cells from the lungs, uterus and spleen of WT and CD18 KO mice following *in vitro* stimulation with PMA/ionomycin/BfA for 4h. n=9 pooled from 3 independent experiments. (C) Cells isolated from WT and CD18 KO tissues were analyzed for V γ chain expression by flow cytometry. Samples were gated on CD3⁺TCR $\gamma\delta$ ⁺ then V γ 1⁺, V γ 4⁺, V γ 5⁺ or V γ 1⁻V γ 4⁻V γ 5⁻. Absolute number of each V γ subset. n=10 pooled from 4 independent experiments. (D) CD18 KO splenocytes were sorted by FACS for CD3⁺ TCR $\gamma\delta$ ⁺ V γ 1⁻ V γ 4⁻ cells then RNA isolated and RT-PCR performed. Representative gels showing expression of V γ and V δ genes. Representative of n=4. Positive controls for each V γ and V δ chain are shown in SI Appendix, Fig. S3C. Statistical differences were determined using a two-way ANOVA. ** $p < 0.01$, **** $p < 0.0001$. Each symbol represents an individual mouse with mean shown.

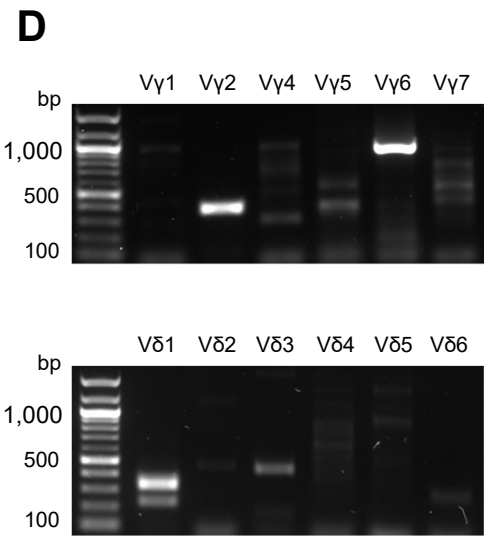
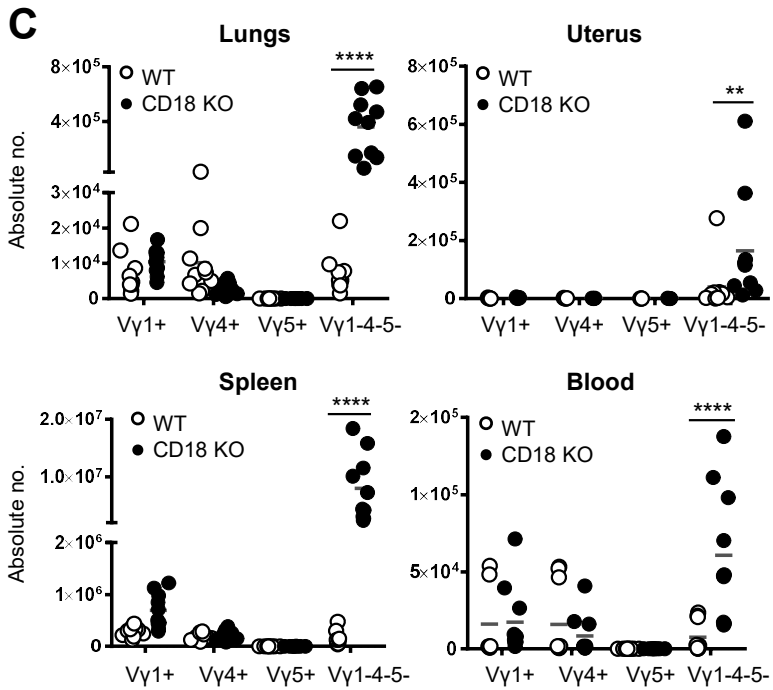
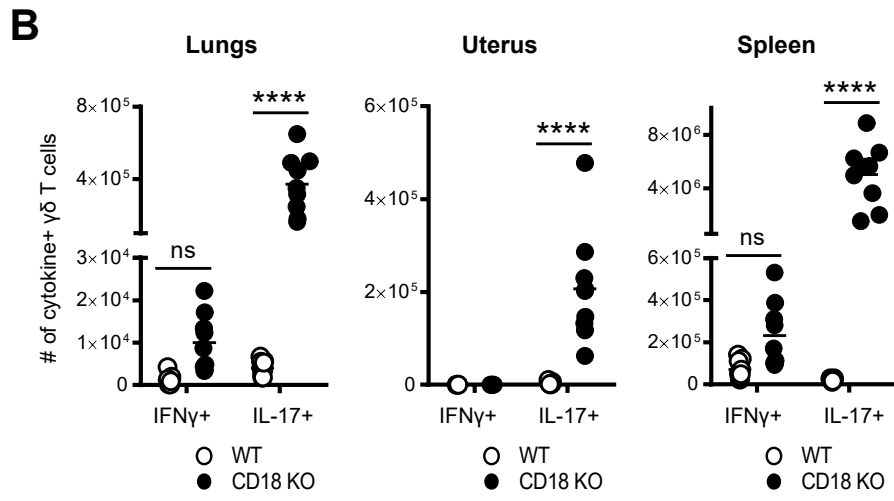
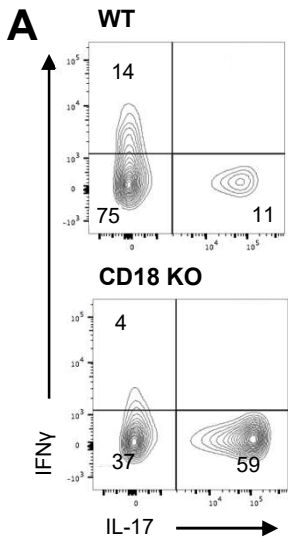
Fig. 3. CD18 KO mice show no difference in V γ 6⁺ thymic development but have impaired development of V γ 4⁺ $\gamma\delta$ T cells. (A-C) Thymocytes were analyzed from E18.5, 1 day, 3 day and 4 week old WT and CD18 KO mice by flow cytometry. Samples were gated on CD3⁺TCR $\gamma\delta$ ⁺ then V γ 1⁺, V γ 4⁺, V γ 5⁺ or V γ 1⁻V γ 4⁻V γ 5⁻ (V γ 6⁺). (A) Absolute number of each V γ subset. (B) Absolute number of V γ 4⁺ and V γ 6⁺ cells gated on either immature CD24⁺ (left) or mature CD24⁻ (right). (C) Absolute number of mature CD24⁻ V γ 4⁺ $\gamma\delta$ T cells gated on either CD27⁺ or CD27⁻. (D) Absolute number of V γ 4⁺ and V γ 6⁺ $\gamma\delta$ T cells from lymphoid tissues of adult mice. pLN = peripheral lymph nodes (inguinal, brachial and axillary pooled); medLN = mediastinal lymph node; mLN = mesenteric lymph nodes. (A-C) n=6-11 pooled from a minimum of 3 independent experiments. (D) pLN, mLN and bone marrow n=9, data pooled from 3 independent experiments. medLN n=6, data pooled from 2 independent experiments. Each symbol represents an individual mouse. Statistical differences were determined using a two-way ANOVA. * $p < 0.05$, ** $p < 0.01$, and *** $p < 0.001$.

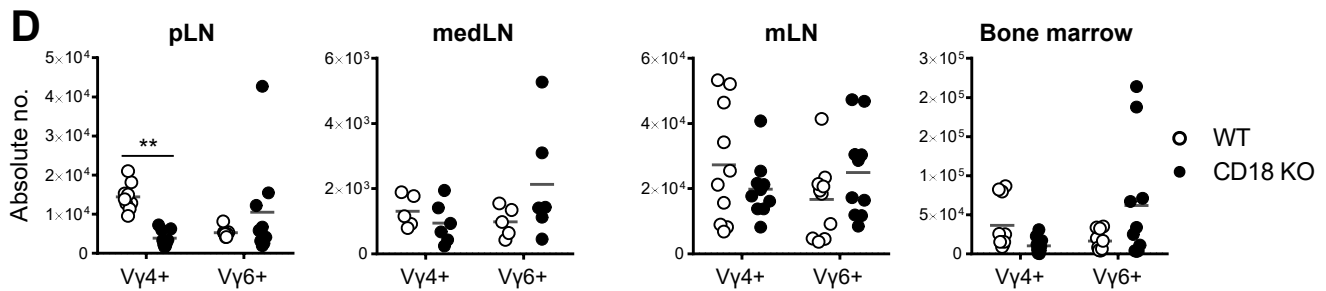
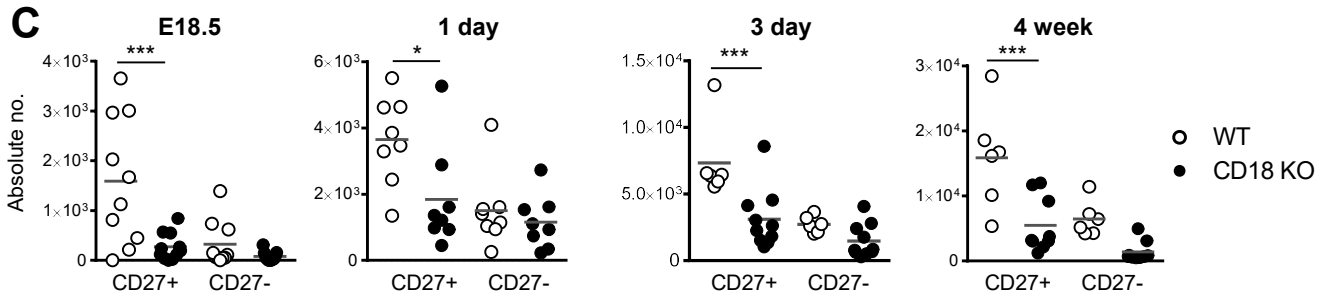
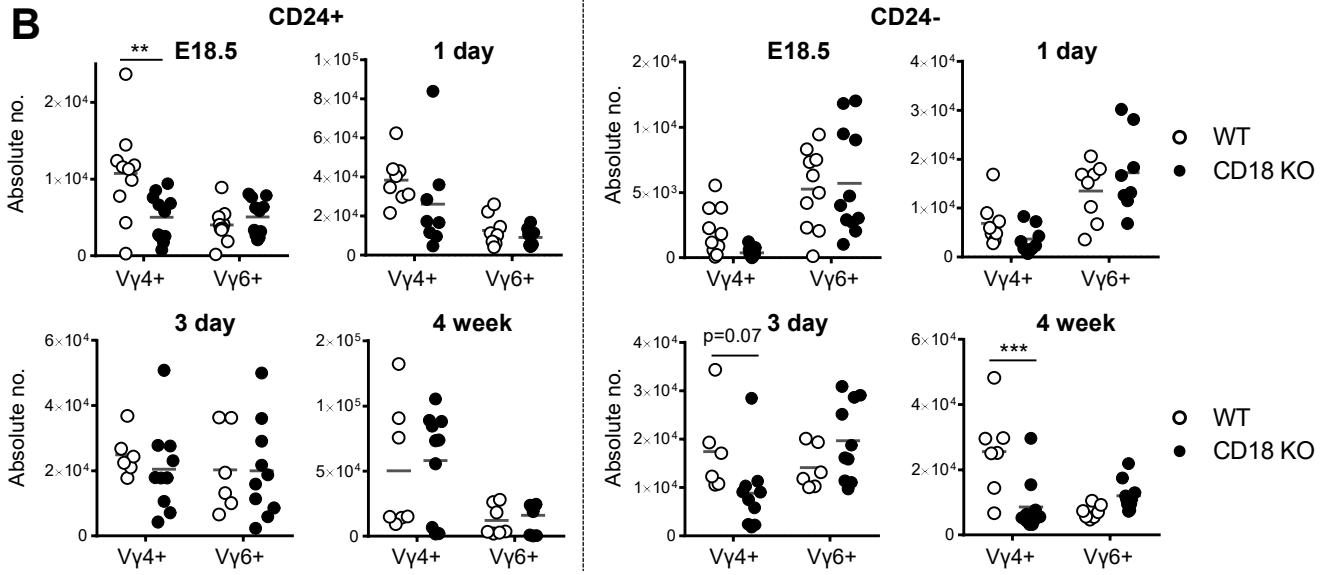
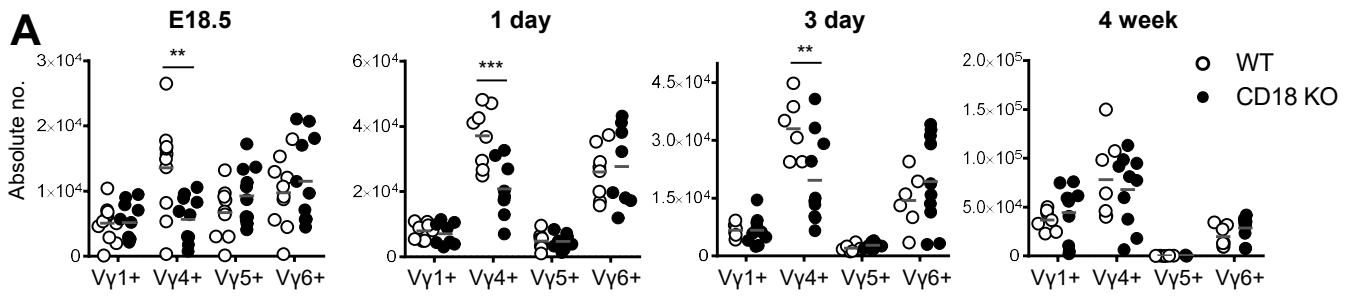
Fig. 4. Single cell RNA sequencing reveals enhanced expression of genes known to negatively regulate apoptosis, specifically in V γ 6⁺ cells from CD18 KO mice. $\gamma\delta$ T cells were purified from the lungs of 2 WT and 1 CD18 KO mice by FACS. scRNAseq was performed and data analyzed as described in detail in the Materials and Methods section. The number of cells sequenced were: WT1, 918 cells; WT2, 6315 cells; KO, 4034 cells. (A) Principal component analysis plot showing the 5 identified clusters. (B) Frequency of cells in each of the identified clusters. (C) Venn diagram showing the shared and unique differentially expressed genes between WT and KO in the 3 major clusters, namely *I117a*⁺, *Ccr7*⁺ and *Ly6c2*⁺. (D) The apoptosis pathways identified in GO enrichment analysis of the differentially expressed genes unique to the *I117a*⁺ cluster. Fold enrichment and p-value are shown for each pathway. +ve = positive; -ve = negative; reg. = regulation; PCD = programmed cell death. (E) Expression levels of selected genes identified by pathway analysis as associated with the negative regulation of leukocyte apoptosis.

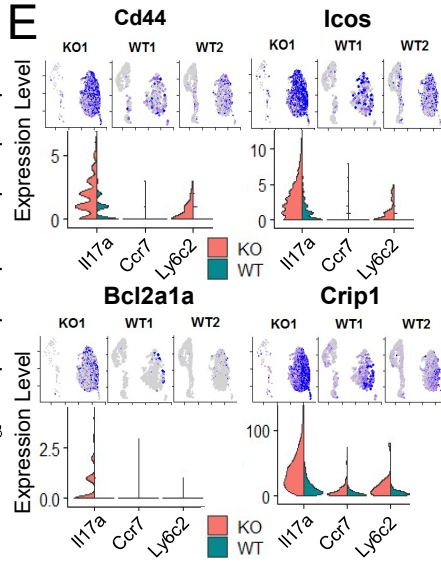
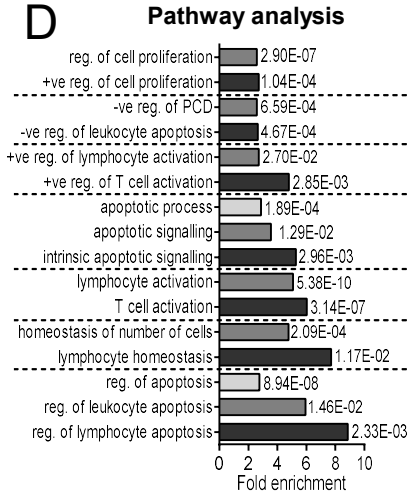
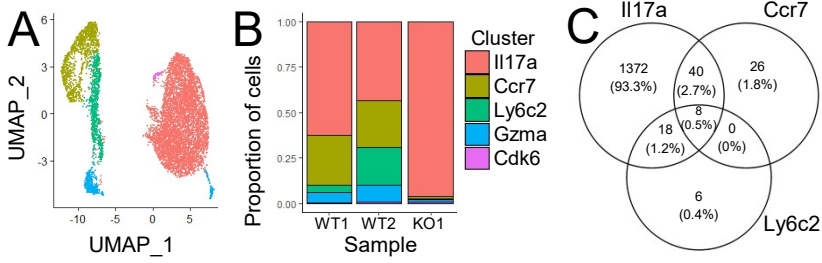
Fig. 5. No evidence of enhanced proliferation in V γ 6⁺ γ δ T cells from CD18 KO mice. (A) Cells isolated from the spleen and lungs of WT and CD18 KO mice were stained for the expression of Ki67. Representative histograms are shown from the spleen. Pooled data shows n=6 from 2 independent experiments. (B) WT and CD18 KO mice were injected with 1mg BrdU i.p. then fed 0.8mg/ml BrdU in the drinking water for 7 days. Cells isolated from the spleen and lungs were analyzed by flow cytometry for expression of BrdU. Representative histograms are shown from the spleen. Pooled data shows n=6 from 2 independent experiments. +ve = positive control (thymus). Each symbol represents an individual mouse. Statistical differences were calculated using a two-way ANOVA, *p<0.05, **p<0.01.

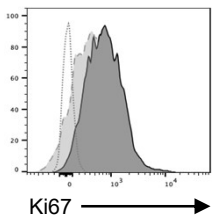
Fig. 6. CD18 KO V γ 6⁺ γ δ T cells display enhanced survival. (A) Analysis of γ δ T cells from the lungs and spleen of WT and CD18 KO mice at various ages. Cells were gated on CD3⁺ TCR γ δ ⁺ then V γ 1⁺, V γ 4⁺, V γ 5⁺ or V γ 1⁻V γ 4⁻V γ 5⁻ (V γ 6⁺). Absolute number of V γ 6⁺ (V γ 1⁻V γ 4⁻V γ 5⁻) γ δ T cells is shown. Where significant differences between WT and CD18 KO were found, the fold difference is shown. WT spleen & lungs at 3 day old n=6. CD18 KO spleen at 1 day old, WT/CD18 KO lungs, WT/CD18 KO spleen at 4 week old, WT lungs 4 week old n=7. WT spleen at 1 day old n=8. CD18 KO spleen at 3 day old, CD18 KO lungs 3 days/4 weeks old, WT spleen E18.5 n=10. CD18 KO spleen & lungs E18.5 n=11. Data pooled from 4-6 litters, with each litter run as an independent experiment, each symbol represents an individual mouse. Statistical differences were determined using a Student's *t* test with false discovery rate approach two-stage linear step-up procedure of Benjamini, Krieger and Yekutieli. (B) Cells isolated from adult WT and CD18 KO lungs and spleen were analyzed by flow cytometry for expression of apoptosis markers. Cells were gated on CD3⁺ TCR γ δ ⁺ then V γ 4⁺ or V γ 1⁻V γ 4⁻ (V γ 6⁺). Proportions of V γ 6⁺ or V γ 4⁺ γ δ T cells that were live (Annexin V⁻ 7AAD⁻), early apoptotic (Annexin V⁺ 7AAD⁻) or late apoptotic (Annexin V⁺ 7AAD⁺) are shown. Graphs show n=9 pooled from 3 independent experiments; each symbol represents an individual mouse. (C) Viable cells (staining negative for viability dye) were calculated in each γ δ T cell subset at various ages of mice. N is as described in (A). (D) CD11a expression in lung and spleen γ δ T cell subsets was quantified by flow cytometry. n=8; 3 independent experiments. Statistical differences were determined using a two-way ANOVA. NS not significant, *p<0.05, **p<0.01, ***p<0.001, ****p<0.0001.





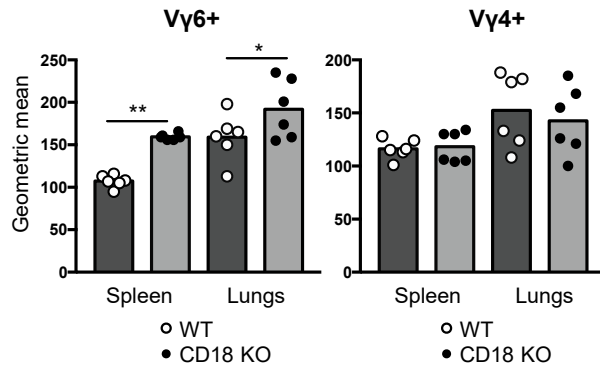
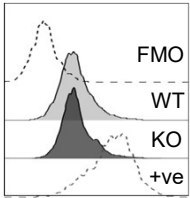




A

Ki67

□ FMO
 □ WT
 ■ CD18 KO

**B**

BrdU

